NATIONAL ADVISORY COMMITTEE FOR AERONAUTICS

TECHNICAL NOTE 3581

EXPERIMENTAL INVESTIGATION OF BLADE FLUTTER IN AN ANNULAR CASCADE

By J. R. Rowe and A. Mendelson

Lewis Flight Propulsion Laboratory
Cleveland, Ohio

Washington
November 1955

NATIONAL ADVISORY COMMITTEE FOR AERONAUTICS

TECHNICAL NOTE 3581

EXPERIMENTAL INVESTIGATION OF BLADE FLUTTER IN AN ANNULAR CASCADE

By J. R. Rowe and A. Mendelson

SUMMARY

The stall operating region of an annular cascade was investigated under varied conditions of geometry and air flow. Controlled variables were angle of attack, blade chord and spacing, number of blades in the cascade, and air velocity. Geometric angle of attack was varied between 0° and 65° with air flows to 500 feet per second. Several blades in each cascade were equipped with strain gages to determine stress, phasing, and flutter frequency. Pressure probes and hot-wire anemometers were used to trace air flows and fluctuations in the test section.

Stall flutter was the only flow phenomenon observed. Rotating stall, which often occurs during stalled operation of many compressors, was not observed although attempts were made to obtain it. Test results indicate that vibratory stress peaks sharply at an angle of attack immediately above the peak mean stress (constant bending stress upon which the vibratory stress is superimposed). This is also approximately the angle of minimum aerodynamic damping. Thus, the decreased damping at stalling angle of attack allows the blades to vibrate sporadically with high stresses under the minor random flow fluctuations of the air stream. Some serious vibratory stresses are shown to exist even prior to blading stall. Many blades had to be replaced in the cascade as tests continued and blades fatigued to fracture. It appears that the peak stresses are increased with increased chord. Decreased blade spacing tended to raise the angle of attack at which stress peaks occur. There was no constant phasing between any blades; the flutter amplitudes were sporadic and unpredictable with respect to time. The blades fluttered in the fundamental bending mode practically to the exclusion of other modes.

INTRODUCTION

Compressor-blade failures by material fatigue have been prevalent since the inception of the gas-turbine engine. As pressure ratios, particularly in axial-flow machines, have increased in newer aircraft-engine compressors, the problem of blade failures has become more acute.

This increase in blade failures has been associated with compressors of high compression ratio operating at off-design speeds.

Forces contributing to fatigue are for the most part aerodynamic. The aerodynamic excitation may be due to many causes, such as classical bending-torsion flutter, shock stalling flutter (ref. 1), choking flutter (ref. 1), rotating stall (refs. 2 to 6), stall flutter (ref. 1), etc.

Classical flutter at low angles of attack is not likely to occur in compressors because of the relatively large stiffness of compressor blades. Shock flutter, which occurs at, or just above, the drag critical Mach number (Mach number at which the pressure rise through the cascade no longer increases with Mach number), and choking flutter, which occurs at certain angles of attack under choking conditions, have been reported in cascade tests (ref. 1). There have been no reports as yet of the occurrence of these types of flutter in full-scale engines.

The phenomenon of rotating stall is presently receiving a great amount of attention (refs. 2 to 6). A rotating-stall field can cause destructive vibrations of the blades if one of the natural frequencies of the blade is in resonance with the frequency of the stall zones passing the blades, or with one of the harmonics of this frequency. Investigations on present-day service engines (ref. 7) have shown blade vibrations caused by rotating stall to be one of the major causes of engine failures.

Stall flutter can occur at high angles of attack when the blade stalls. It is indicated in reference 2 that stall flutter has occurred in compressors simultaneously with rotating stall. Private communications received by the authors have indicated the existence of serious stall-flutter vibrations without the occurrence of rotating stall in experimental, high-air-capacity compressors of advanced design utilizing blades of relatively low stiffness in the early stages. Stall flutter is defined herein as an aerodynamically excited vibration at high angle of attack that is not due to periodic flow fluctuations.

The aerodynamically excited vibrations in an annular cascade simulating a compressor stage were studied in this investigation. The use of such a stationary annular cascade makes it possible to study easily the effects of changing various parameters such as angle of attack, air velocity, stagger angle, solidity, etc. The results of experiments on such a cascade for various values of the parameters indicated are presented herein. Aerodynamic damping was computed using the method of reference 8. A correlation was obtained between the vibratory stress and the aerodynamic damping.

APPARATUS

Facilities

The wind tunnel (fig. 1) used for investigating the cascade characteristics reported herein had the following major components and dimensions:

(1) The test-section enclosure used one section of a 19-inch-diameter jet-engine compressor case, which allowed removal of the upper half for inspection and changing of the cascade and instrumentation.

(2) Fine mesh screen and a sheet of Fiberglas inserted across the middle of a surge tank (length, 10 ft; diam, 4 ft) upstream of the test section served to produce a pressure drop and straightening effect on the flow. Straightening tubes were also added between the tank and the test enclosure.

(3) The hub in the test section had a 13-inch-length, projecting, bullet nose piece and 18-inch-length, stinger tail piece. The straight portion of hub was 10 inches long and 9.5 inches in diameter.

(4) The entire hub assembly was supported by four low-drag struts from tail piece to tunnel wall.

(5) The atmospheric outlet of the tunnel was covered with a 5/8- by 5/8-inch heavy mesh screen to stop broken cascade blades, etc. from leaving the tunnel.

(6) Two air-flow control valves were mounted far upstream of the test section.

Cascade and Turning Vanes

Cascade geometry, which remained constant throughout this study, included

(1) Untapered, untwisted blades

(2) Airfoil section typical of a conventional jet-engine compressor

(3) Airfoil length of 4.5 inches

(4) Cascade hub (steel) of 9.5 inches diameter

(5) Axial centerlines of blade roots radial in hub

All cascades were made of airfoils machined from 2024-T (24S-T) aluminum. To minimize root-fixture damping, a number 2 Morse taper was used to facilitate root tightening. Changes in cascade geometry for increasing the scope of this study were made by having two hubs (23 and 30 blade spacings) and two airfoil chord sizes (fig. 2) of 1.25 and 1.75 inches. The fundamental bending frequencies for the 1.25- and the 1.75-inch blades were 200 and 255 cycles per second, respectively.

Turning vanes provided uniform turning of the incoming air across the span of the airfoils in cascade. These vanes were located roughly 3 chord lengths upstream of the cascade. Forty sheet Inconel (1/16 in.) vanes were tack-welded between a hub and flush-to-case shroud to form the turning set. Air entered the cascade at an angle of about 53° with the tunnel axis.

Instrumentation

Two constant-current hot-wire anemometers were used employing radial, transverse, or both radial and transverse mountings of 0.001-inch sensing wire in the probes. Signals from the hot wires were displayed on a dual-beam oscilloscope. Electronic filters eliminated high-frequency noise.

To check the turning effect of the stator and cascade sections on the air, pressure probes were utilized. Both hot-wire anemometers and pressure probes could be moved circumferentially and radially by motor actuators controlled from a remote panel in the control room.

Electrical resistance strain gages (500 ohms, active part 1/4 by 1/8 in.) were attached with quick-setting cement to several blades in each cascade. These gages were mounted on the suction airfoil surface as near the root as possible, with the active part of the gage directed along the span. Lead wires fed through a drilled hole in the root and into the hub junction box. All gage leads passed from the box through the hub supports out of the tunnel to the control room. Blades equipped with strain gages were inserted into the hub so that adjacent or diametrically opposite, or both, blade traces could be compared simultaneously on a four-channel strain analyzer.

Both hot-wire-anemometer and strain-gage traces were photographed by 35-millimeter oscillo-record cameras. Four gage traces could be viewed simultaneously on the analyzer-oscilloscope at gains up to 20,000.

Tunnel inlet-air temperature was indicated by thermocouple output calibrated in degrees Fahrenheit on a potentiometer pyrometer.

A low-frequency audio-oscillator signal was added to a crystal pickup signal for determining the individual blade frequencies by using Lissajous figures on the oscilloscope. A pulsating air stream, and/or a violin bow were used to excite single blades for obtaining the natural frequencies of the blades.

PROCEDURE

All blades in the cascade were adjustable for varying the angle of attack. Prior to each test run, the blades were set by hand to the desired angle. The complete range of geometric angle of attack investigated varied from 0° to 65°.

In order to determine the mean stress, the position of the strain-gage null signal at zero air flow was recorded on film; then the air flow was started and slowly increased to the desired flow level. After flow had become constant, records were taken of the new trace mean position. The calibration factor between deflection of trace on oscilloscope and stress in the blade being known, the mean stress was determined. Vibratory stresses were determined from the amplitude of the vibratory trace. A 10-power viewer aided in reading the correct strain amplitudes from the film.

Maximum vibratory and mean stress variation with air velocity through the cascade (keeping angle of attack constant) was of considerable magnitude. For comparison purposes, test data were taken for all points keeping air velocity constant throughout the desired range of angle of attack. All points making up either the mean-stress or vibratory-stress curves were determined under similar flow conditions in which the velocity through the cascade was about 345 feet per second.

In all tests, the inlet-air temperature and static and dynamic pressures were recorded at the same time as the oscillo-records were being taken. Usually the air-flow angles at the cascade inlet and outlet were measured by claw- or wedge-type probes and balancing U-tube manometers to check the turning effect of the vanes and cascade.

RESULTS AND DISCUSSION

Stalling flutter was the only flow phenomenon observed in this investigation that contributed to the cyclic stressing of the blades in the annular cascade. Vibratory stresses of large magnitudes were encountered as the angle of attack of the blades was increased to the stall region. An example of typical strain-gage signals is shown in figure 3. The vibrations are not of constant amplitude, but sporadically build up and taper off. This sporadic change of amplitude occurred in all the

tests made, and the data presented in the subsequent figures are all based on the maximum stress occurring for, at least, three consecutive cycles.

The maximum vibratory stress measured by strain gages is shown in figures 4(a) and (b) for a constant inlet-air velocity of 345 feet per second. Cascades of 30 blades with 1.25- and 1.75-inch chords were investigated over a range of angle of attack. These chords correspond to solidities at the midspan of 0.84 and 1.17. The maximum vibratory stress increased to a sharp peak of ±10,000 to ±12,000 psi as the angle of attack was increased, and then decreased rapidly with further increase in angle of attack. A similar curve for the 1.25-inch chord is shown in figure 4(c) for an air velocity of 500 feet per second. The peak vibratory stress for this velocity was approximately ±21,000 psi. The maximum stresses measured are not necessarily the maximum stresses in the blades, since the strain gages were not generally located at the maximum stress point. As a result of this high vibratory-stress region, the endurance limit (approximately 16,000 psi) of the 2024-T blades was much exceeded. This caused many blade fractures throughout the test program.

The increase and subsequent decrease in vibratory stress with angle of attack can be explained on the basis of the stalling of the cascade as the angle of attack was increased and the subsequent recovery of some of the lift. This can be seen more clearly in figure 5 where the ratio of the mean stress to maximum mean stress is plotted against angle of attack for the two sets of blades previously discussed. The ratio is plotted since it is only the shape of the curve which is of interest here. The mean stress is taken as a measure of the mean lift acting on the airfoil, and it is seen that the shape of the curve is typical of the lift curve for many airfoils. At the very high angles of attack, the strain gages will include a component of strain due to airfoil drag, and, thus, the curve does not necessarily show quantitatively correct lift in the region.

It appears that vibratory stress reaches a maximum in the vicinity where the lift curve has a maximum negative slope. Comparison of figures 5(a) and (b) with 4(a) and (b) shows that vibratory stress increased rapidly as the airfoil stalled. These figures indicate that the peak vibratory stress occurs approximately at that angle of attack for which the slope of the lift curve has a maximum negative value; as the lift on the airfoil begins to recover, the vibratory stress drops.

It has been known for many years (ref. 9) that if an airfoil oscillates in the stall region, the aerodynamic forces acting on the airfoil tend to lag the motions, producing a hysteresis curve and enabling the airfoil to absorb sufficient energy from the air stream to maintain its oscillations. Using such a hysteresis effect made it possible in reference 8 to account for the decrease in aerodynamic damping, and, thus, for

the decrease in critical flutter air velocity at stall. This was done by assuming that the angle of aerodynamic lag, as it was called, was proportional to the change in slope of the lift curve from a straight line. Although this assumption neglects the fact that the dynamic lift curve of an airfoil can differ considerably from the static lift curve, it enables one to obtain a qualitative measure of the aerodynamic damping in the stall region.

Such a calculation on the aerodynamic damping was performed by using figure 5(a) to obtain the angle of aerodynamic lag. (The details of the calculation are given in the appendix.) The results are shown in figure 6 for the cascade of 1.25-inch-chord blades. Shown in the figure is the variation of the ratio of the aerodynamic damping to the aerodynamic damping at zero angle of attack (herein referred to as damping factor) with angle of attack. It can be seen from this figure that the damping drops almost to zero. A comparison with figure 4(a) reveals the peak vibratory stress to occur at the angle of attack where the aerodynamic damping is a minimum.

Figure 7 is an example of the manner in which the dimensionless vibratory stress varied with the damping factor for the data derived from tests on the 30-blade cascade with 1.25-inch chords. Figure 7 was obtained by cross-plotting figures 4(a) and 6. The maximum relative stress occurs concurrently with minimum aerodynamic damping.

Possible phasing between adjacent blades in the annular cascades was investigated using cascades of even (30) and odd (23) numbers of blades. Simultaneous strain-gage traces from the cascade blades showed no constant phasing in either case. Each blade vibrated at or near its own natural frequency in every case. Vibration amplitudes varied timewise in a sporadic and unpredictable manner. This trait of the vibration mechanics only served to prevent further any continuity in phasing. Thus, there was no evidence of constant or periodic phasing between blades. No constant blade phasing resulted from changes in angle of attack, solidity, chord length, or air velocity through the cascade.

The sporadic nature of the vibrations can possibly be explained on the basis of the damping curve of figure 6. Since the damping becomes very low in the stall region, any minor, sporadic fluctuations in the air stream will cause the blades to vibrate. These vibrations, however, will not persist unless the damping is sufficiently negative. Thus, there results a constant building up and tapering down in vibration amplitude. The results reported herein indicate that vibrations in the stall region under these conditions can be of sufficiently large magnitude to cause blade failures. Although this vibration differs from classical constant-amplitude flutter, it results from a decrease in aerodynamic damping. This type of vibration, although not a true flutter vibration, is similar to that discussed in reference 1 and designated as stall flutter.

Throughout this investigation, major flutter amplitudes occurred in the first fluxural mode of the blade (also evidenced by the fatigue pattern of fig. 8); however, from time to time there appeared second and/or third flexural frequency traces superimposed upon the fundamental. At other infrequent times during the relative nulls in the fundamental trace, the second bending mode appeared with an amplitude approximating 20 percent of the maximum fundamental amplitude elsewhere in the trace; the third bending amplitude was never significant. No evidence of torsional oscillations was observed in this investigation. Figure 8 shows the "fatigued" cross section of one blade; the fatigue pattern clearly indicates the predominantly flexural deformation.

Sisto (ref. 10) has indicated that "decreased blade spacing is ... beneficial in delaying the onset of stall-flutter toward higher incidences." This trend was verified in these annular cascades as shown by comparison of figures 4(a) and 9. However, increasing the solidity by holding spacing constant and increasing the blade chord produced the flutter peaks at a lower value of angle of attack than was the case prior to chord modification. The condition incorporating increased blade chord is illustrated by comparison of figures 4(a) and (b). From what has been done it appears that blade spacing and blade-chord variables may have independent effects on the flutter angle, so long as other dimensions and influences are kept constant.

It is to be noted (figs. 4(a) and (b)) that the vibratory stress peak of the blades with 1.75-inch chord is higher than that for the blades of 1.25-inch chord. Change in solidity by increased spacing of blades (for example, reducing the number of blades in the cascade from 30 to 23) also produced a higher vibratory stress peak (fig. 9). These trends also indicate that blade spacing and blade chord may have independent effects on magnitude of peak stresses as well as angle of attack at which they occur.

The effect of stagger on either blade stresses or the position of peak stresses with respect to angle of attack was not determined, since only one set of turning vanes (nominal turning angle, 53° from axial) was used in this investigation. British cascade tests (ref. 1) indicate a widening of the band of severe flutter as the stagger angle increases.

Rotating stall was not encountered at any time during this investigation. Some experimental data indicate that a static-pressure rise is necessary to produce rotating stall. In an effort to obtain rotating stall, an attempt was made to separate the effects of the pressure drop through the turning vanes and the subsequent pressure rise through the cascade into independent energy systems by successively moving the turning vanes 5 and then 15 chord lengths upstream of the cascade. These efforts were unsuccessful.

SUMMARY OF RESULTS

The stall operating region of an annular cascade was investigated under varied conditions of geometry and air flow.

Vibratory stress as well as mean stress in cascade blading was observed to be dependent upon the angle of attack of the blading to the air flow and the velocity of the flow (holding other parameters and physical factors constant).

Aerodynamic damping dropped sharply at the onset of blading stall and permitted the rapid, high peaking of vibratory stresses. It appears that the vibratory stress reaches a maximum in the vicinity where the lift curve has a maximum negative slope.

Flutter amplitude was sporadic throughout the investigation and offered no indication of constant or periodic phasing between blades of the cascade. The blades fluttered at their individual natural frequencies. The fundamental bending mode of vibration predominated the observed oscillations.

Decreased blade spacing tended to raise the angle of attack at which the peak stall flutter occurred. However, these preliminary tests also show a reduction in the angle of attack at which peak stall flutter takes place with increase in blade chord. More data are needed from more physically different cascades to substantiate either or both of these initial indications.

Lewis Flight Propulsion Laboratory
National Advisory Committee for Aeronautics
Cleveland, Ohio, August 31, 1955

APPENDIX - DETERMINATION OF AERODYNAMIC DAMPING FACTOR

Aerodynamic damping variation with geometric angle of attack is plotted in figure 6. The damping term was derived from the theory and procedure presented in reference 8. That presentation defined the following symbols; they are presented here for this example of computation of the aerodynamic damping factor:

C_L dimensionless lift coefficient

S_m measured mean root stress

α angle of attack

α_0 angle of attack at zero lift

α_g geometric angle of attack (angle between blade chord and inlet air)

φ angle of lag between displacements or velocities and aerodynamic restoring or damping forces, deg

$\cos \varphi$ aerodynamic damping factor

In reference 8 the angle of aerodynamic lag (as corrected) was assumed to be given by

$$\varphi = 360 - K\left[\left(\frac{dC_L}{d\alpha}\right)_{\alpha=\alpha_0} - \left(\frac{dC_L}{d\alpha}\right)\right]$$

where, with φ being degrees, $K = 45/2\pi$. Then, the quantitative aerodynamic lag may be determined from

$$\varphi = 360 - \frac{45}{2\pi}\left[\left(\frac{dC_L}{d\alpha}\right)_{\alpha=\alpha_0} - \left(\frac{dC_L}{d\alpha}\right)\right]$$

To determine the value of $dC_L/d\alpha$ in the preceding equation, use is made of the mean stress curve in figure 5(a). It is assumed that C_L is proportional to the mean root stress. To obtain the constant of proportionality, the slope $\left(\frac{dS_m}{d\alpha}\right)_{\alpha=\alpha_0}$ is measured. The constant of proportionality is then that value by which $\left(\frac{dS_m}{d\alpha}\right)_{\alpha=\alpha_0}$ must be multiplied in order to obtain the correct value of $\left(\frac{dC_L}{d\alpha}\right)_{\alpha=\alpha_0}$, this value being

approximately 2π for an isolated airfoil and less than 2π (ref. 11) for airfoils in cascade. Using this constant yields the values of $dC_L/d\alpha$ for any α from the measured values of $dS_m/d\alpha$. This method therefore requires a knowledge of $\left(\frac{dC_L}{d\alpha}\right)_{\alpha=\alpha_0}$ for the given cascade.

Garrick in reference 11 derives the theoretical lift coefficient for blades in cascade. For the cascades of the present investigation, the applicable form for C_L is

$$C_L = 4\frac{g}{C}\frac{\sin \alpha_x}{(\cosh^2 \gamma_0 - \sin^2 \beta)^{1/2}}$$

where C equals the blade chord, g is the spacing between blade chords, α_x is the sum of the aerodynamic angle of attack and the blade chord setting angle β measured from the tunnel axis. The quantity $\cosh \gamma_0$ is a function of g/C and β, and is tabulated in reference 11. For the 30-blade cascade with 1.25-inch-chord blades, g/C becomes 1.2, and $\beta_{\alpha=\alpha_0}$ equals 48.4° for this airfoil and inlet-air angle combination. The value of the initial slope of the lift curve may then be computed as approximately 5.9 for this particular cascade system.

For this example of calculation of damping factor, a geometric angle of attack of 16° will be used. Substitution of the value of mean stress slope (corrected to initial slope of 5.9) from figure 5(a) produces

$$\varphi_{\alpha_g=16^\circ} = 360 - (45/2\pi)(5.9 - 3.0) = 339^\circ$$

and

$$\cos \varphi = 0.93$$

The damping force that corresponds to the out-of-phase component of the lift is proportional to the $\cos \varphi$ as can be obtained from equation (3) of reference 8 for the case of pure bending. The $\cos \varphi$ is therefore considered to be the damping factor as plotted in figure 6.

REFERENCES

1. Kilpatrick, D. A., and Ritchie, J.: Compressor Cascade Flutter Tests - 20° Camber Blades, Medium and High Stagger Cascades. C.P. No. 187, British A.R.C., 1955.

2. Pearson, H.: The Aerodynamics of Compressor Blade Vibration. Fourth Anglo-American Aero. Conf. (London), Sept. 15-17, 1953, pp. 127-162; discussion, pp. 162A-162J. (Publ. by Roy. Aero. Soc. (London).)

3. Sears, W. R.: On Asymmetric Flow in an Axial-Flow Compressor Stage. Jour. Appl. Mech., vol. 20, no. 3, Sept. 1953, pp. 442-443.

4. Huppert, Merle C., and Benser, William A.: Some Stall and Surge Phenomena in Axial-Flow Compressors. Jour. Aero. Sci., vol. 20, no. 12, Dec. 1953, pp. 835-845.

5. Emmons, H. W., Pearson, C. E., and Grant, H. P.: Compressor Surge and Stall Propagation. Trans. A.S.M.E., vol. 77, no. 4, May 1955, pp. 455-467; discussion, pp. 467-469.

6. Marble, Frank E.: Propagation of Stall in a Compressor Blade Row. Tech. Rep. No. 4, GALCIT, Jan. 1954. (Office Sci. Res., Air Res. and Dev. Command Contract AF 18(600)-178.)

7. Johnsen, Irving A.: Some Considerations in Axial-Flow Compressor Design. Vol. III of Aircraft Propulsion, NACA-Univ. Conf. on Aero., Construction, and Propulsion, Oct. 20, 21, and 22, 1954.

8. Mendelson, Alexander: Aerodynamic Hysteresis as a Factor in Critical Flutter Speed of Compressor Blades at Stalling Conditions. Jour. Aero. Sci., vol. 16, no. 11, Nov. 1949, pp. 645-654.

9. Studer, Hans-Luzi: Experimental Investigations Concerning Wing Flutter. Trans. No. 58, A.A.F., Air Materiel Command, Wright Field Intelligence Div., May 23, 1942.

10. Sisto, F.: Flutter of Airfoils in Cascade. Sc.D. Thesis, M.I.T., Sept. 1952.

11. Garrick, I. E.: On the Plane Potential Flow Past a Lattice of Arbitrary Airfoils. NACA Rep. 788, 1944. (Supersedes NACA WR L-313.)

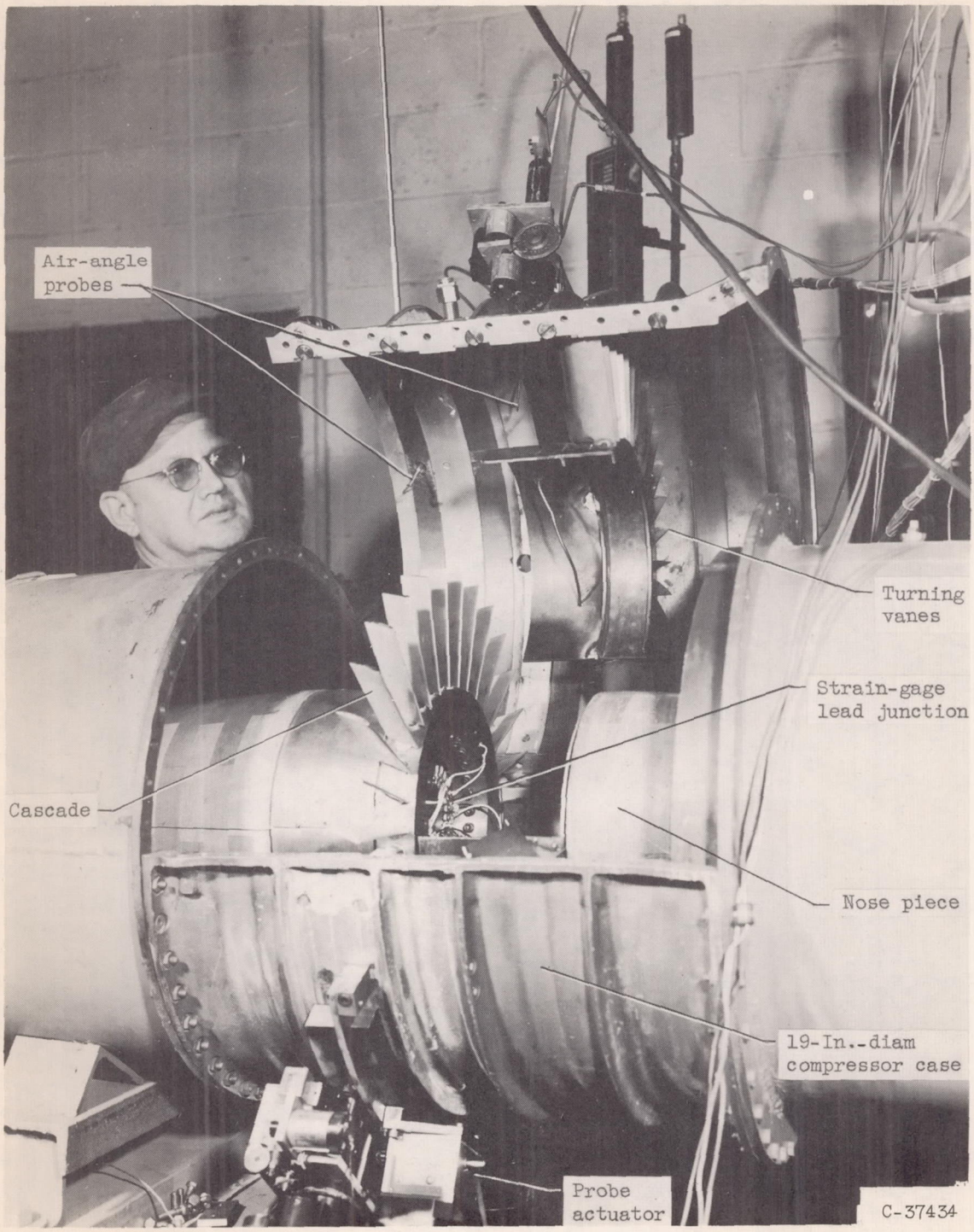

Figure 1. - Wind-tunnel test section with vanes and cascade shown. Air flow to left.

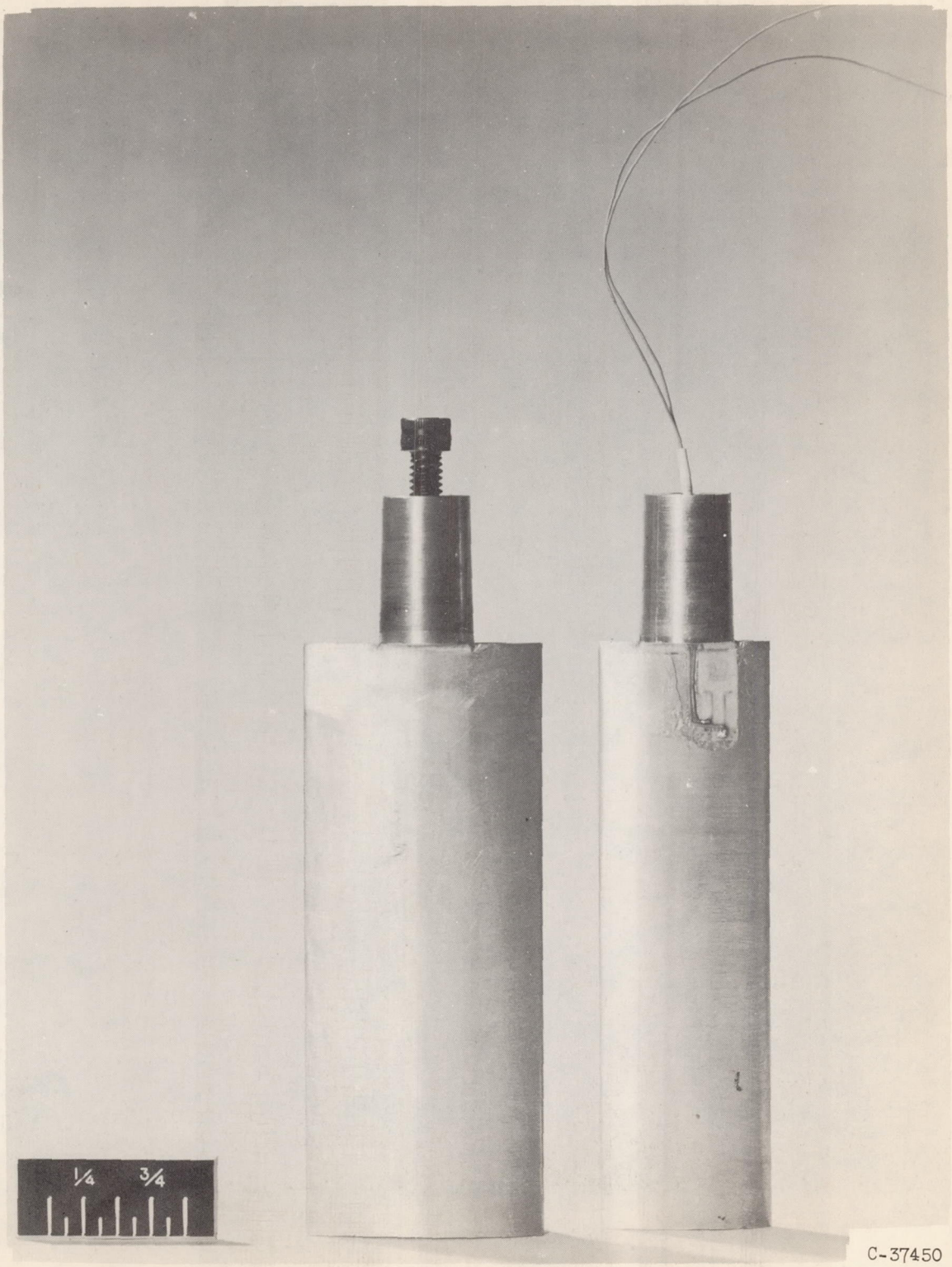

Figure 2. - Cascade blades and strain-gage mounting. Blade chords, 1.75 and 1.25 inches.

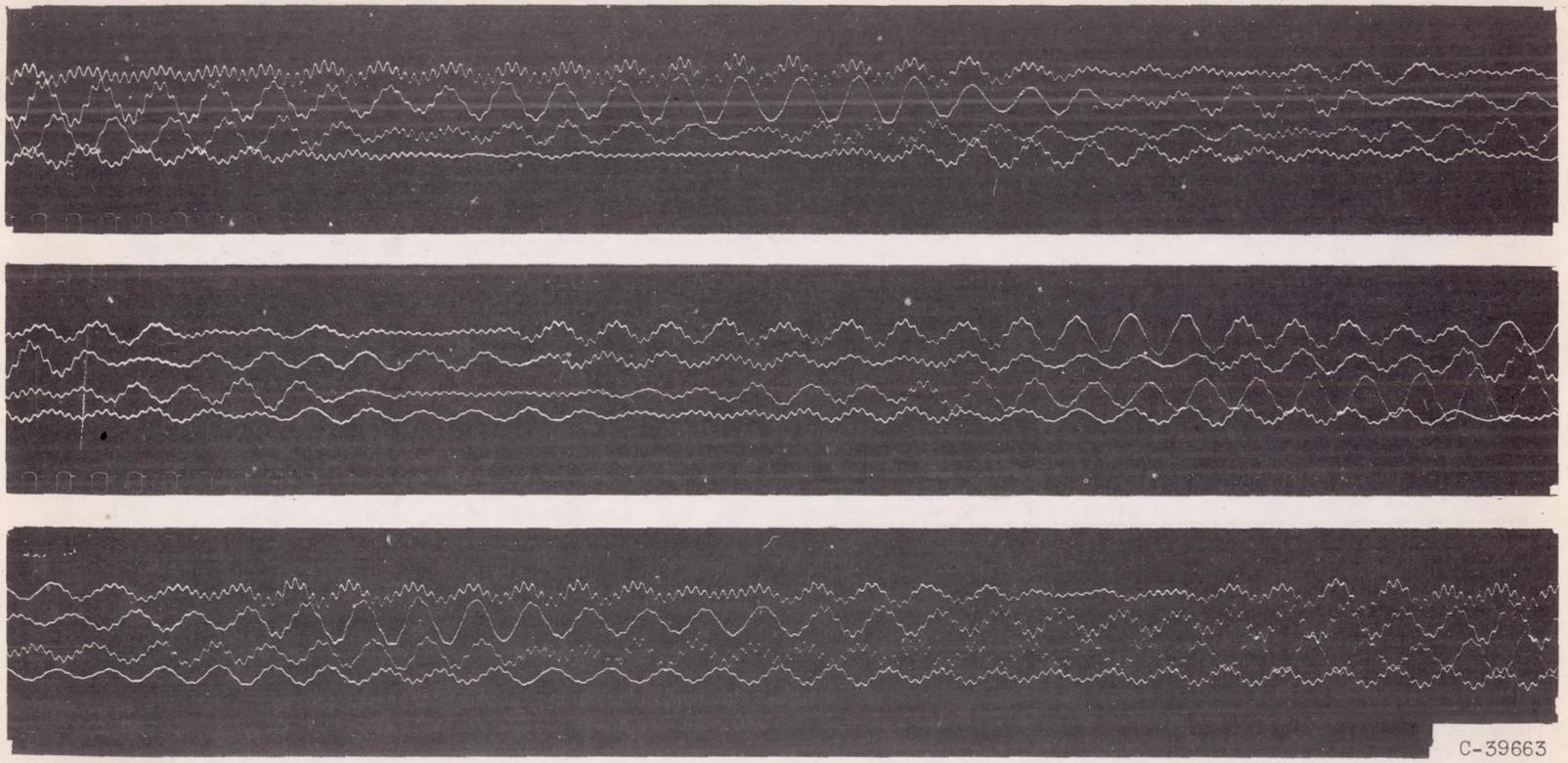

Figure 3. - Simultaneous strain-gage traces of four blades in a 30-blade cascade. Blade chord, 1.25 inches; velocity entering cascade, 500 feet per second; angle of attack, 30°; film speed, 60 inches per second.

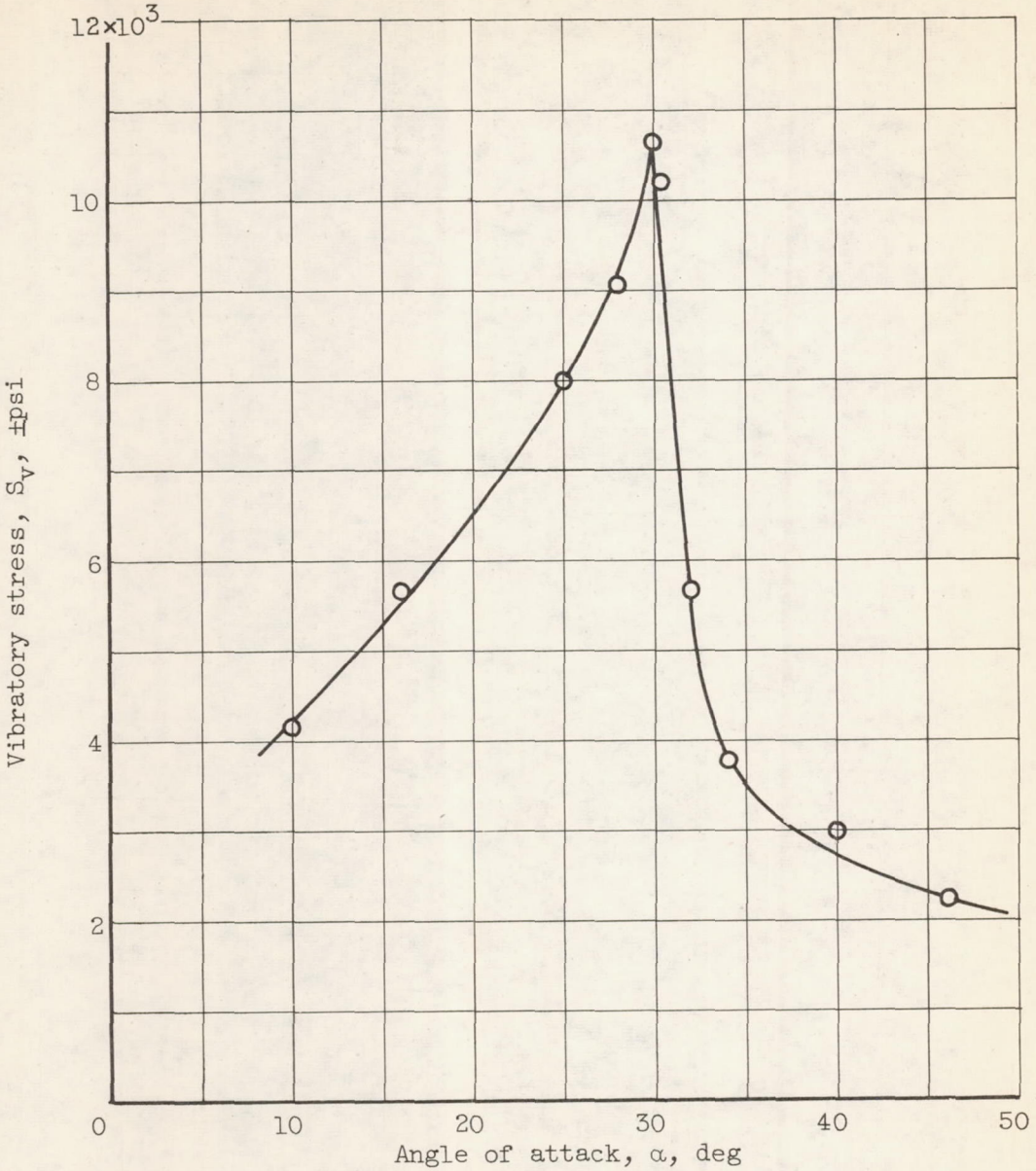

(a) Blade chord, 1.25 inches; velocity entering cascade, 345 feet per second; one-half span solidity, 0.84.

Figure 4. - Variation of vibratory stress with angle of attack in a 30-blade cascade.

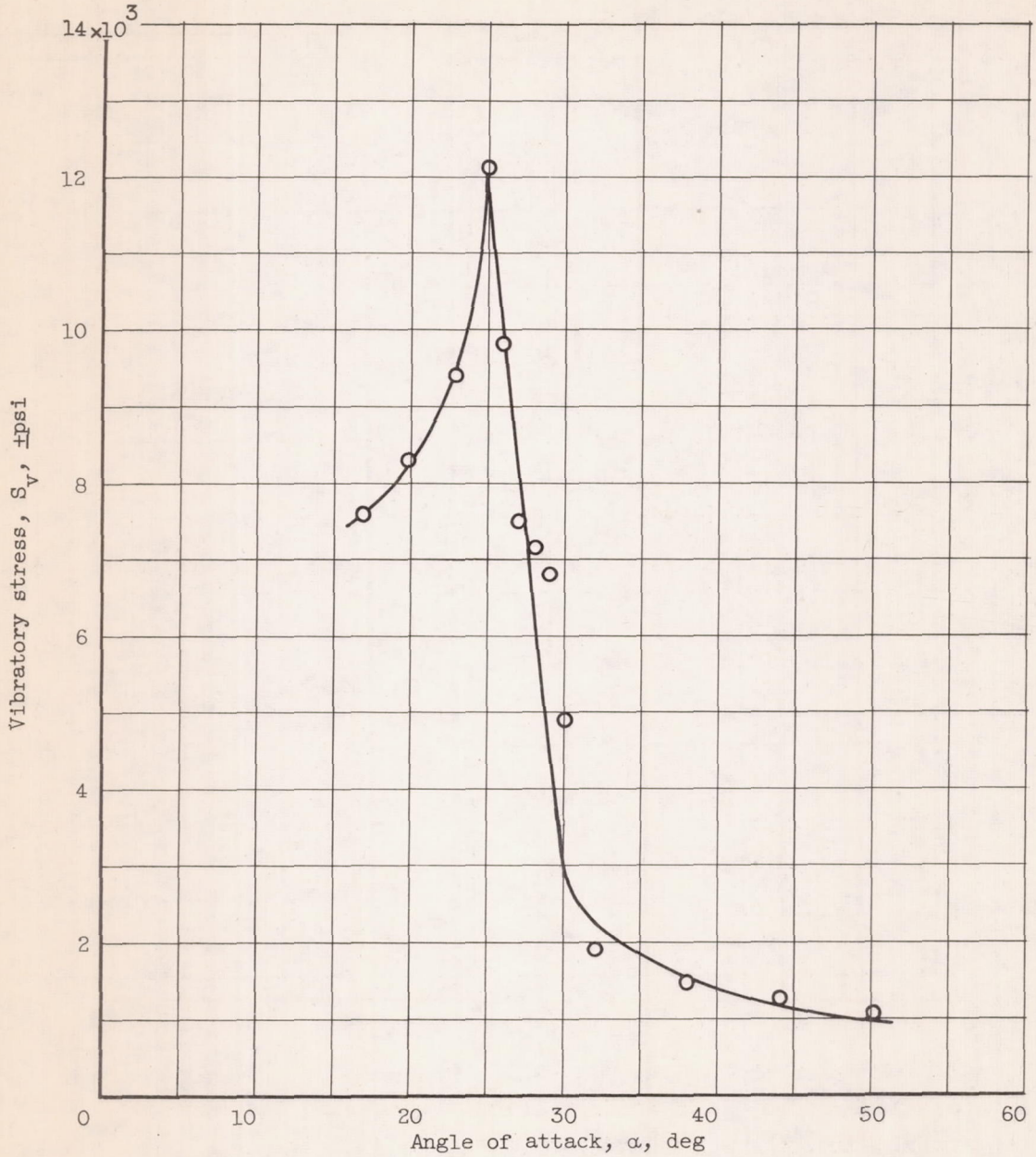

(b) Blade chord, 1.75 inches; velocity entering cascade, 345 feet per second; one-half span solidity, 1.17.

Figure 4. - Continued. Variation of vibratory stress with angle of attack in a 30-blade cascade.

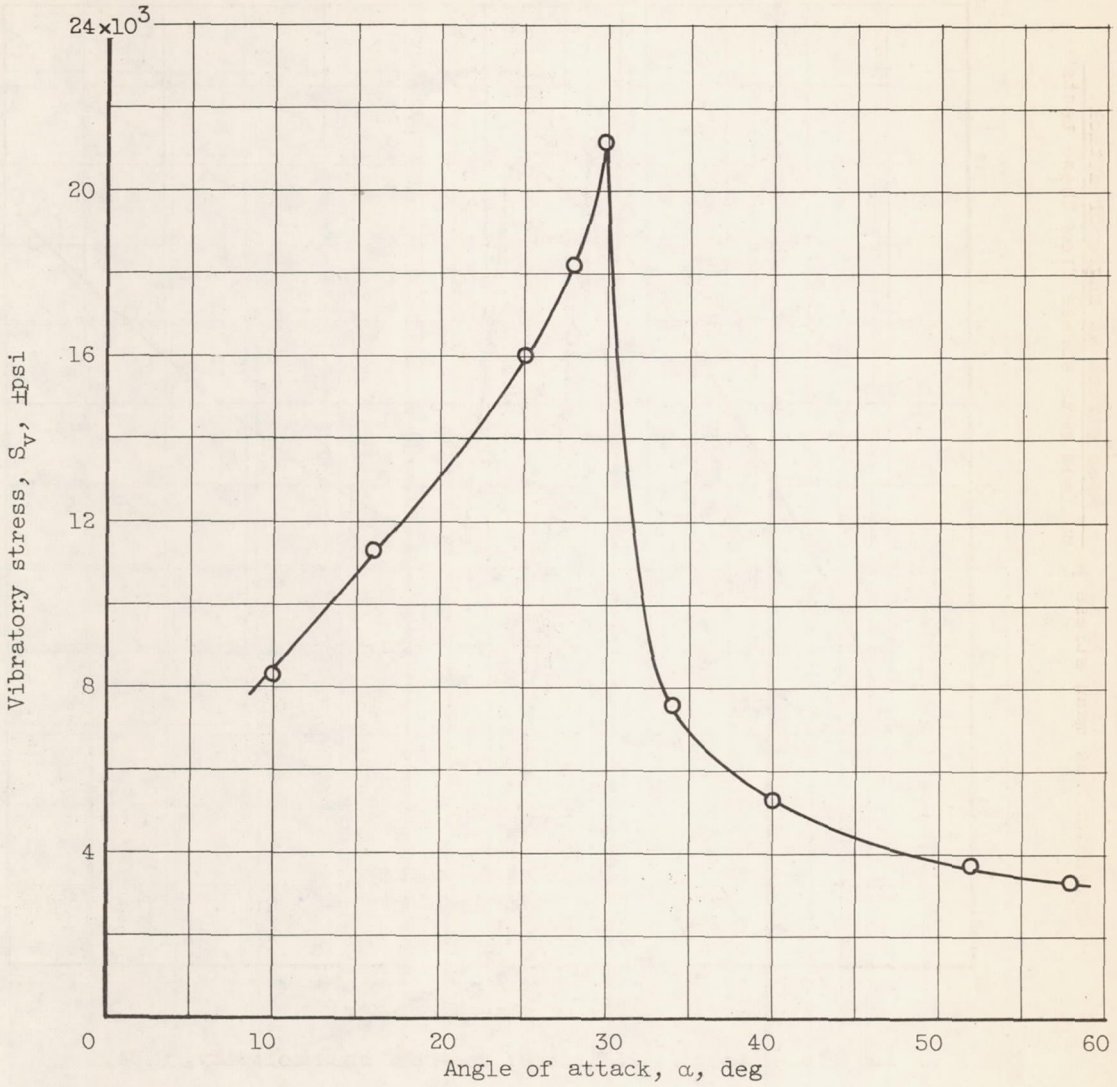

(c) Blade chord, 1.25 inches; velocity entering cascade, 500 feet per second; one-half span solidity, 0.84.

Figure 4. - Concluded. Variation of vibratory stress with angle of attack in a 30-blade cascade.

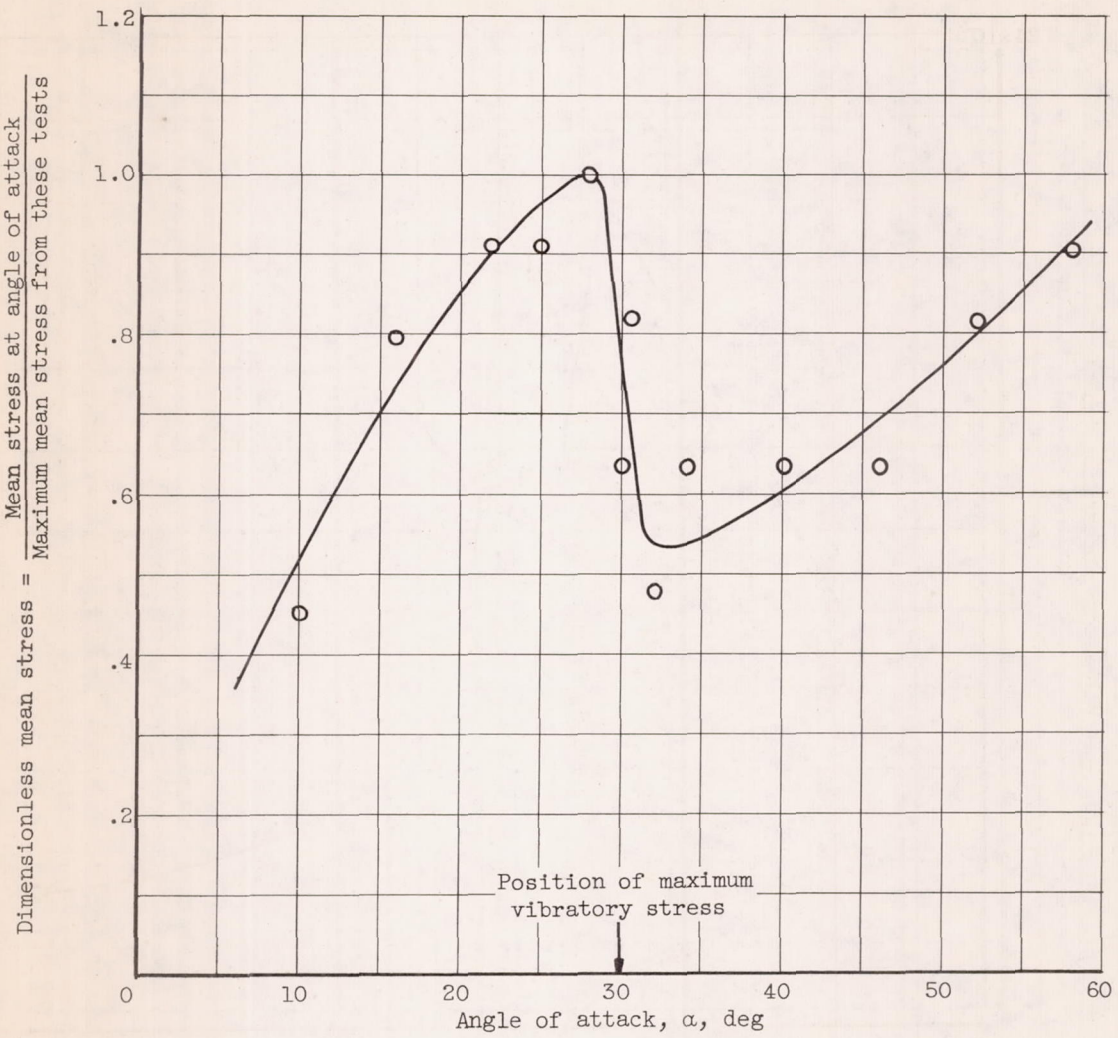

(a) Blade chord, 1.25 inches; one-half span solidity, 0.84.

Figure 5. - Variation of dimensionless mean stress with angle of attack in a 30-blade cascade. Velocity entering cascade, 345 feet per second.

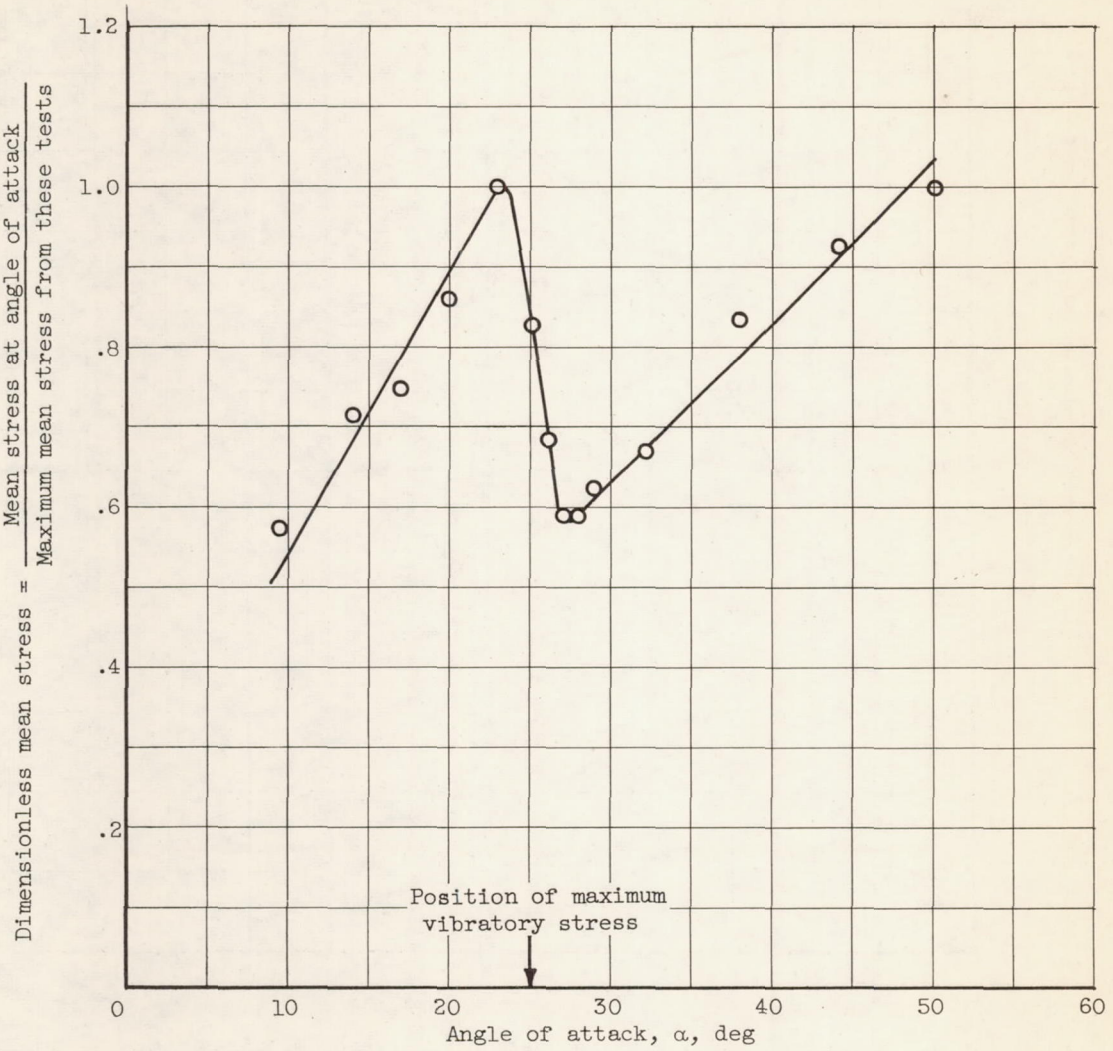

(b) Blade chord, 1.75 inches; one-half span solidity, 1.17.

Figure 5. - Concluded. Variation of dimensionless mean stress with angle of attack in a 30-blade cascade. Velocity entering cascade, 345 feet per second.

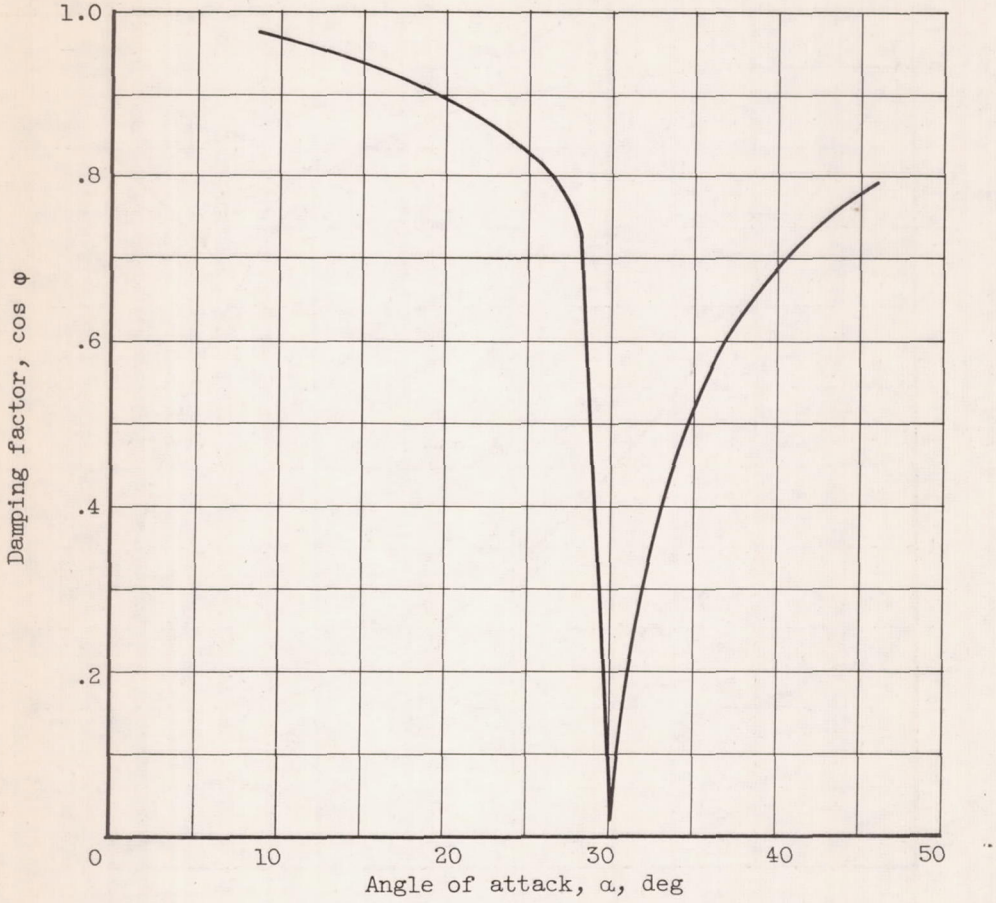

Figure 6. - Variation of damping factor with angle of attack in a 30-blade cascade. Blade chord, 1.25 inches; velocity entering cascade, 345 feet per second; one-half span solidity, 0.84.

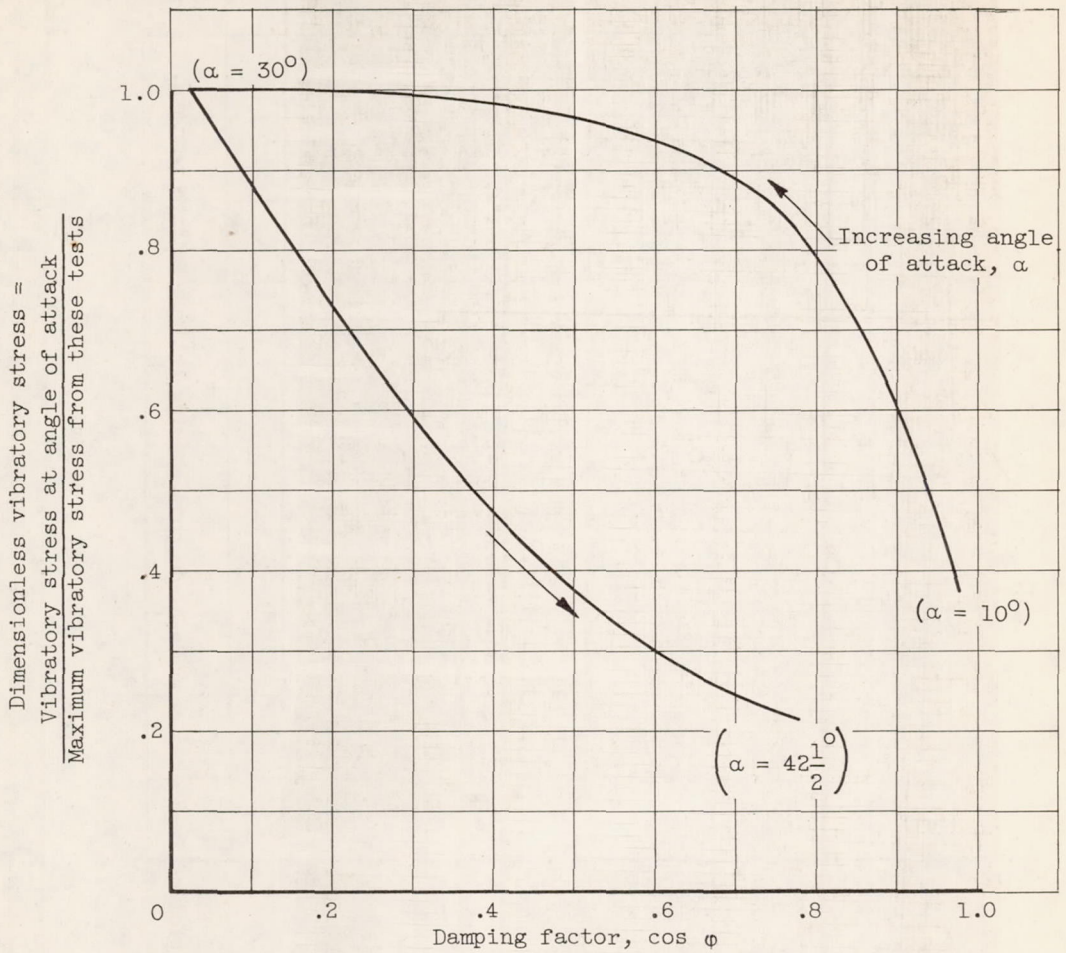

Figure 7. - Variation of dimensionless vibratory stress with damping factor in a 30-blade cascade. Blade chord, 1.25 inches; one-half span solidity, 0.84.

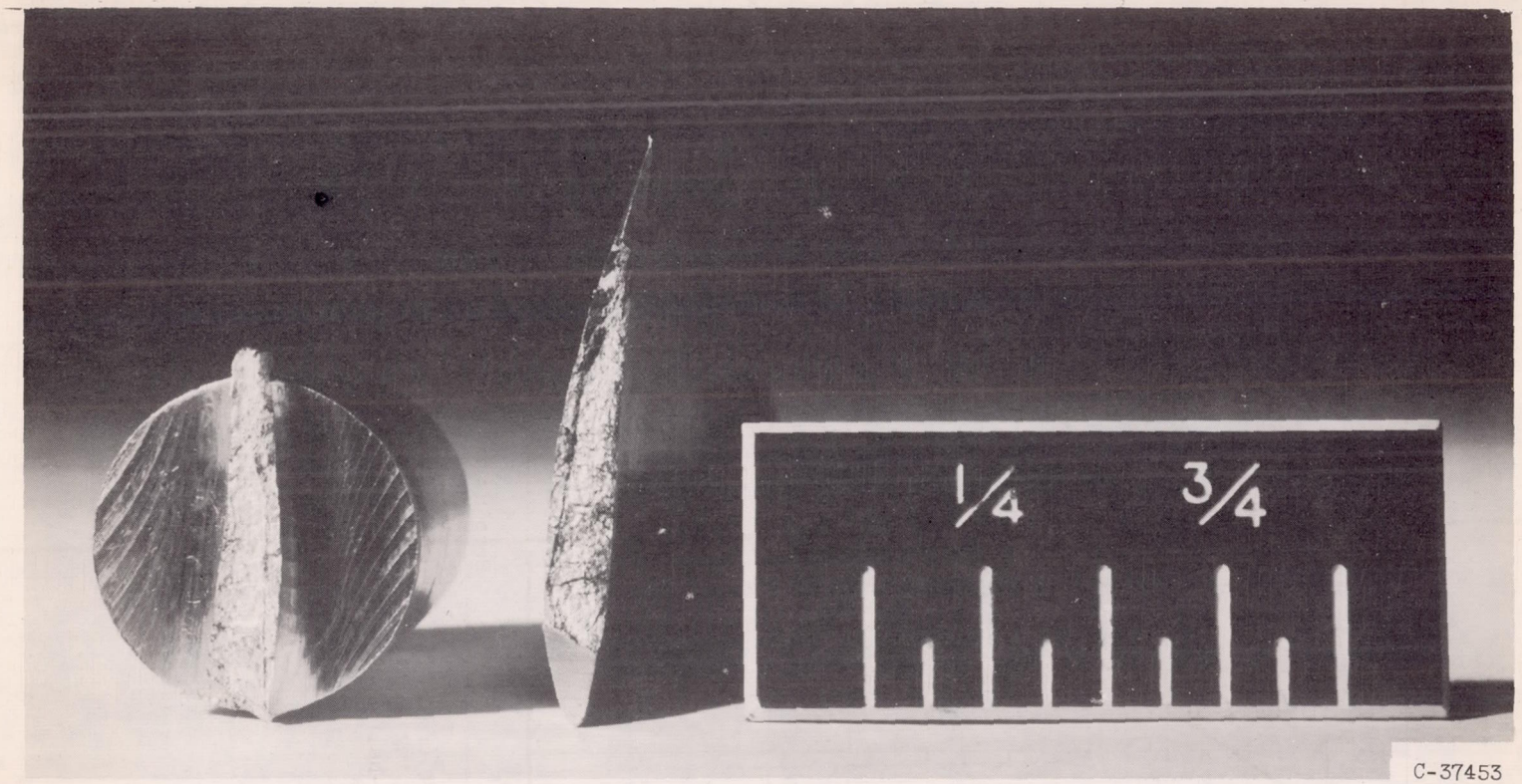

Figure 8. - Cross section of fractured cascade-blade root showing fatigue-failure pattern.

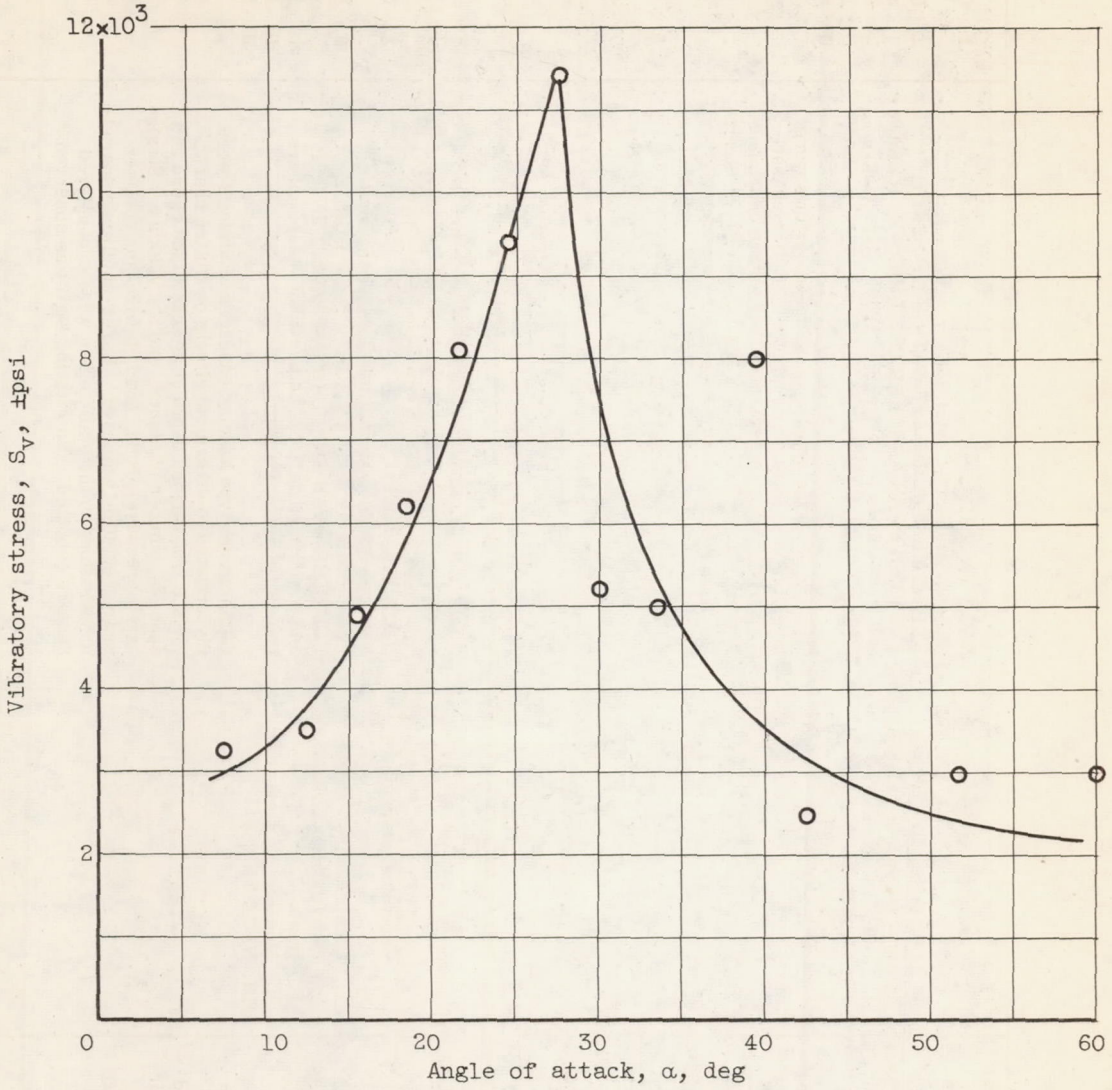

Figure 9. - Variation of vibratory stress with angle of attack in a 23-blade cascade. Blade chord, 1.25 inches; velocity entering cascade, 345 feet per second; one-half span solidity, 0.64.